



# Optical losses in porous silicon waveguides in the near-infrared: Effects of scattering

Patrick Ferrand, R. Romestain

## ► To cite this version:

Patrick Ferrand, R. Romestain. Optical losses in porous silicon waveguides in the near-infrared: Effects of scattering. Applied Physics Letters, 2000, 77 (22), pp.3535. 10.1063/1.1329161 . hal-00272403

**HAL Id: hal-00272403**

**<https://hal.science/hal-00272403>**

Submitted on 15 Apr 2015

**HAL** is a multi-disciplinary open access archive for the deposit and dissemination of scientific research documents, whether they are published or not. The documents may come from teaching and research institutions in France or abroad, or from public or private research centers.

L'archive ouverte pluridisciplinaire **HAL**, est destinée au dépôt et à la diffusion de documents scientifiques de niveau recherche, publiés ou non, émanant des établissements d'enseignement et de recherche français ou étrangers, des laboratoires publics ou privés.

# Optical losses in porous silicon waveguides in the near-infrared: Effects of scattering

P. Ferrand<sup>a)</sup> and R. Romestain

*Laboratoire de Spectrométrie Physique, Université J. Fourier-CNRS (UMR 5588), BP 87, 38402 Saint Martin d'Hères Cedex, France*

(Received 13 June 2000; accepted for publication 2 October 2000)

Benefitting from the long path inside planar waveguides, we have investigated the optical losses of porous silicon, in the continuous 0.8–1.6  $\mu\text{m}$  (0.77–1.55 eV) range. The obtained values, typically a few  $\text{cm}^{-1}$ , are 1 order of magnitude larger than “pure” absorption losses measured previously. The other main sources of loss, including scattering on both interface roughness and nanocrystallites, are invoked. Calculations give the same order of magnitude as measurements. We also detected scattered light close to the direct beam. © 2000 American Institute of Physics. [S0003-6951(00)03548-8]

The discovery of luminescence<sup>1</sup> of porous silicon (PS) at room temperature has initiated a strong research effort concerning the optical properties of this material, resulting in the realization of distributed Bragg reflectors,<sup>2</sup> luminescent microcavities,<sup>3</sup> holographic gratings,<sup>4</sup> and planar waveguides.<sup>5,6</sup> This last application is very promising for gas detection<sup>7</sup> and all-silicon optoelectronic integrated devices.<sup>8</sup>

With these aims, the knowledge of the losses is crucial, especially in the near infrared (NIR) range (0.8–1.6  $\mu\text{m}$ ), where PS becomes relatively transparent. Many authors report quantitative transmission measurements,<sup>9–12</sup> performed perpendicular to the surface of free-standing PS single layers, but only in spectral ranges where losses are relatively high, due to the layer thicknesses that are typically limited to  $\sim 100 \mu\text{m}$ . Photothermal deflection spectroscopy (PDS), based on the thermal gradient adjacent to an irradiated sample,<sup>13</sup> avoids this problem, but gives only the absorption coefficient of the PS,<sup>9,11</sup> ignoring all other sources of losses. Benefitting from the long path inside a waveguide, some authors have estimated the losses in as-formed PS,<sup>5,8</sup> but at a single wavelength.

In this letter, we report quantitative measurements of the transmission in PS, performed in single mode waveguides, in the continuous 0.8–1.6  $\mu\text{m}$  range. Planar waveguides were made by etching two successive layers with different porosities. We used low doped *p* type (100) silicon substrates (4  $\Omega\text{cm}$ ), with a thickness of only 100  $\mu\text{m}$ , to allow perfect cleaved edges. The upper (guiding) layer and the lower (cladding) layer were made using a  $\text{HF:H}_2\text{O:C}_2\text{H}_5\text{OH}$  (35:35:30) solution at room temperature, and current densities of 16.6 and 50  $\text{mA cm}^{-2}$ , in order to obtain respective porosities of 65% and 58%.

Our experimental setup was based on end-fire coupling. Light from a straight tungsten filament was coupled into and out of the sample using two Cassegrain reflecting microscope objectives ( $\times 25$ , numerical aperture=0.4 and  $\times 15$ , numerical aperture=0.28) in order to be perfectly achromatic. Using a beamsplitter, the output edge was imaged

onto both a NIR camera and the entrance slit of a 1200 gr/mm monochromator. The polarization is selected by a polarizer inserted in front of the monochromator. The signal was acquired by a cooled InGaAs photomultiplier, and measured through a lock-in amplifier. All experimental spectra are corrected by the spectral response of the detection system, which is measured by imaging the filament without any sample.

Refractive indices were measured by fitting reflectance spectra of single layers in the 0.25–1.6  $\mu\text{m}$  range.<sup>14</sup> Roughness measurements were performed using a Tencor P-10 surface profiler.

We designed a waveguide allowing the propagation of a quasisymmetric single mode, denoted  $\text{TE}_0$  or  $\text{TM}_0$ , for wavelengths  $\lambda$  larger than 1.3  $\mu\text{m}$ . In order to do this, the guiding layer was 1.5  $\mu\text{m}$  thick, with a refractive index  $n_g=1.77$ , and the 3  $\mu\text{m}$  cladding layer ( $n_c=1.67$  at  $\lambda=1.3 \mu\text{m}$ ) avoids leakage in the high index bulk Si substrate. For shorter wavelengths, a second (asymmetric) mode exists, but it is easy to convince oneself that they cannot be coupled efficiently to the symmetric external field. This point was confirmed experimentally, because we did not observe any interference fringes in our spectra. These are usually the consequence of the propagation of several modes, each one with its own phase velocity, as we have already observed on multimode samples.

Figure 1 shows experimental transmittance spectra performed for both polarizations, on samples of two distinct lengths  $L$ . The picture in the inset is a front view of the horizontal output edge of the waveguide. It shows two illuminated areas, because the central obscuration of the input Cassegrain objective and the numerical aperture of the waveguide do not allow an efficient coupling along the objective axis. The white rectangle represents the relative size of the entrance slit of the monochromator, where only one area of the output edge is imaged on. Since the transmitted light includes effects other than the propagation, like coupling efficiency, it is not possible at this stage to plot absolute transmittance.

Accurate measurements of the absolute losses are deduced from the ratio of intensities transmitted by samples of

<sup>a)</sup>Author to whom correspondence should be addressed; electronic mail: patrick.ferrand@ujf-grenoble.fr

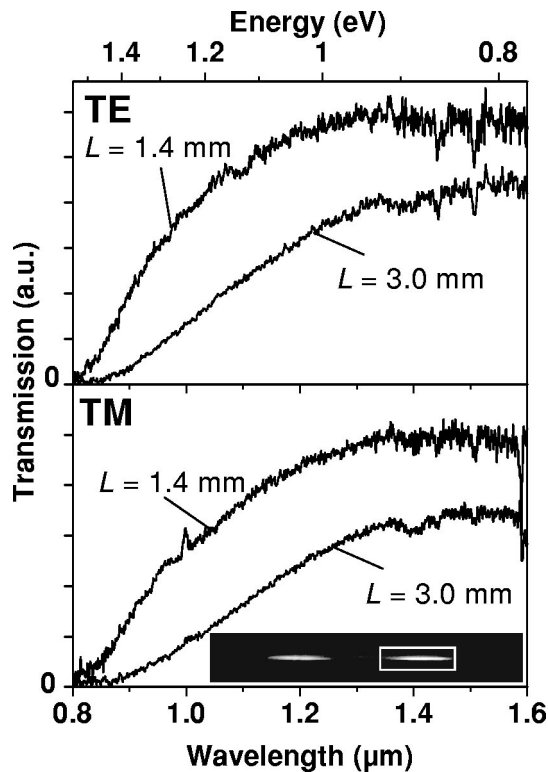


FIG. 1. Transmission spectra of PS waveguides of different length  $L$ , for TE (top) and TM (bottom) polarizations. The inset is a front view of the horizontal output edge, and the white rectangle represents the relative size of the monochromator slit, whose length is adjusted to cover all the illuminated area.

different lengths. Taking care that the image of the illuminated area of the output edge is always shorter than the entrance slit, the differences in intensity can only be attributed to the difference in path lengths. The obtained values are plotted in Fig. 2. We also report “pure” absorption coefficient measurements, performed by Vincent *et al.* on  $p$  type PS,<sup>9</sup> and by Daub *et al.* on low doped  $p$  type bulk silicon.<sup>15</sup> Vincent *et al.* attribute the sub-band gap absorption to the probable presence of tail states, in volume or in surface. Our

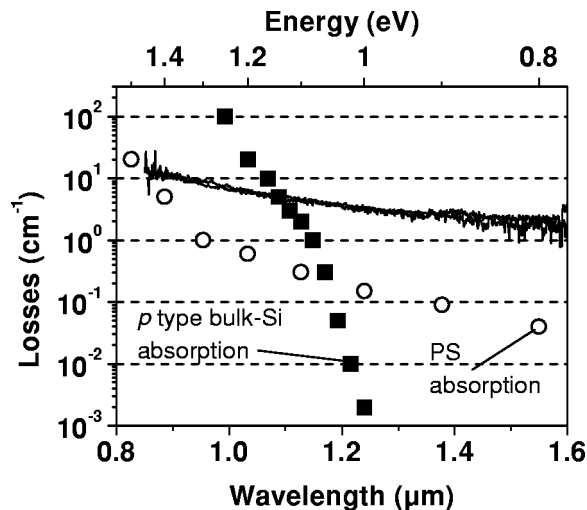


FIG. 2. Spectral dependence of the absolute losses, deduced from the transmission spectra of Fig. 1. Values obtained for both polarizations are perfectly superposed. Optical absorptions of PS, measured by PDS, and of bulk Si are also plotted.

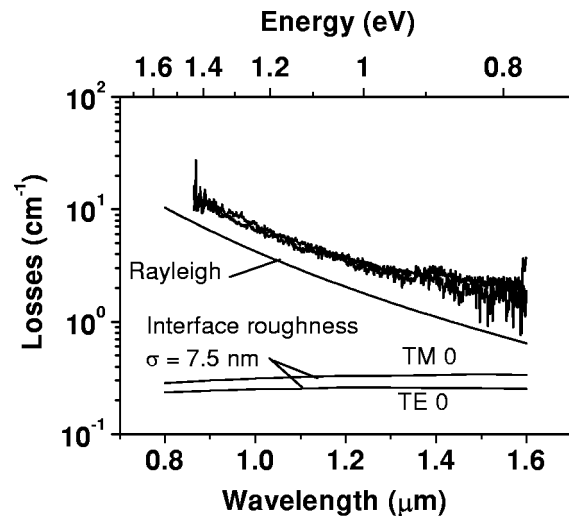


FIG. 3. Comparison between measured losses and calculated possible sources of losses: scattering on the bottom interface roughness or on Si nanocrystallites.

measurements follow the same decrease steadily with increasing wavelengths, but the obtained values are typically 1 order of magnitude larger than the PS optical absorption, especially for large wavelengths.

This clearly suggests other strong sources of loss. We considered leakage to the bulk-Si substrate, scattering by the interface roughness, or by the randomness of the nanocrystallites. Calculated losses are obtained by solving rigorously the Maxwell equations in the whole structure by means of a transfer matrix formalism for an incident plane wave coupled into the waveguide by a prism coupler, like  $m$ -line experiments.<sup>16</sup> Losses have the same consequences as the imaginary part  $\kappa_g$  of the guiding optical index. They can be evaluated by monitoring the linewidth of the guided mode, assuming that the propagation losses  $\alpha$  are given by  $\alpha = 4\pi\kappa_g/\lambda$ , as they are in a bulk material.

Due to the finite thickness of the cladding layer, the leakage into the high index substrate occurs, especially for large wavelengths. In our case, the waveguide has been designed to minimize this kind of loss, and the largest value, calculated for  $\lambda = 1.6 \mu\text{m}$  in TM polarization, is only  $8 \times 10^{-2} \text{ cm}^{-1}$ .

The interface roughness, localized in the case of  $p$  type PS at the bottom of each PS layer,<sup>14</sup> is a well known source of small angle scattering losses.<sup>17</sup> By etching only a single layer of same thickness and porosity as the guiding one, and then by dissolving it in NaOH (0.1 M), the root mean square deviation to the planarity  $\sigma$  at this bottom interface has been directly measured. We found  $\sigma = 7.5 \text{ nm}$ . In our case, the correlation length of the surface variation is long compared to the wavelength.<sup>17</sup> The Fresnel coefficients at this interface is thus corrected<sup>18</sup> by the factor  $\exp[-8(\pi\sigma n_g \cos \theta_g/\lambda)^2]$ , where  $\theta_g$  is the angle inside the guiding layer. Global calculations performed as described above give losses plotted versus wavelength on Fig. 3. These losses are relatively constant, near  $0.3 \text{ cm}^{-1}$ , in our spectral range, because the direct dependence with  $\lambda$  is compensated by the continuous variation of  $\theta_g$  with  $\lambda$ .

Finally, the nanoporous structure of  $p$  type PS gives strong spatial fluctuations of the dielectric constant. The re-

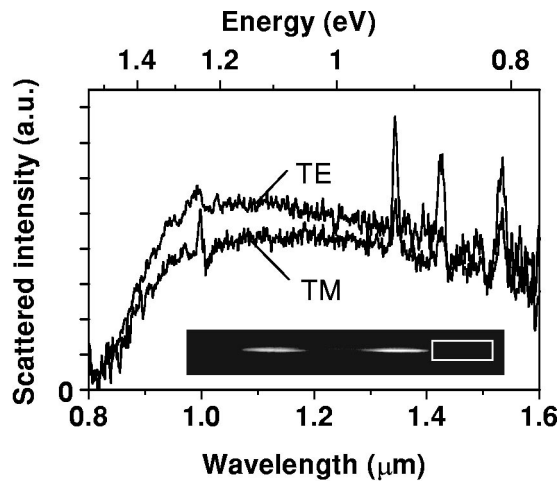


FIG. 4. Scattered intensity measured near the transmitted beam in the guiding plane.

sulting Rayleigh scattering loss coefficient  $\alpha$ , in the case where the index deviations are small and extended over regions small compared to the wavelength, can be written as<sup>19</sup>

$$\alpha_{\text{Rayleigh}} = \frac{8\pi^3}{3\lambda^4} \langle (n_g^2 - \bar{n}_g^2)^2 \rangle v_c, \quad (1)$$

where  $\langle (n_g^2 - \bar{n}_g^2)^2 \rangle$  is the variance of the permittivity  $n_g^2$  and  $v_c$  a correlation volume. The dielectric properties of Si nanocrystallites are an open area of investigations, and their descriptions need the use of complex models.<sup>20</sup> We are aware that the crude model of Si spherical crystallites of 4 nm<sup>21</sup> of index 3.5, is outside the domain of validity of Eq. (1), however we plotted the estimated losses on Fig. 3. The obtained values are in the same range as our measurements.

In order to bear out experimentally the scattering process, we also studied the outcoming light near the direct output beam. We could measure detectable intensities (typically 2 orders of magnitude lower), only very close to the direct beam, and along the guiding plane. The results are plotted in Fig. 4. The integrating area is shown on the inset. Ignoring the three peaks in the 1.3–1.6  $\mu\text{m}$  range, which might be attributed to a possible resonant scattering of some chemical species inside the PS, the spectral dependence is quite different from the one observed on the direct transmitted light. Light scattered in the 0.8–1.0  $\mu\text{m}$  range suffers both strong absorption and strong scattering, and it cannot be measured. The evolution for larger wavelengths shows decreasing efficiency for larger wavelengths, confirming the interpretation of a scattering process.

These measurements show that the propagation of light in PS waveguides is perturbed by several sources of losses. Two main types of processes contribute to losses: “pure” absorption, which is weak in the NIR range, and scattering, which represents an important part of our measured losses. Unfortunately, our measurements did not allow us to separate the respective roles of volume and surface scattering. Quantitative measurements of scattered power are difficult; they require the determination of its angular distribution, particularly in the radiated and guided modes.

However, the obtained values of a few  $\text{cm}^{-1}$  are promising for optoelectronic integrated devices in the NIR range. In order to reduce these losses, many groups use oxidized porous silicon, and they obtain losses as weak as  $0.25 \text{ cm}^{-1}$ , also in the visible range,<sup>22</sup> but unfortunately the oxidation does not preserve the large range of optical index in PS, required by photonic structures. A promising way to reduce the interface roughness is to perform the PS anodization at low temperature.<sup>23</sup>

In conclusion, we have performed quantitative measurement of transmission in the PS waveguide, in the continuous 0.8–1.6  $\mu\text{m}$  range. The obtained losses have been compared for several sources of loss, including absorption, leakage, interface, and volume scattering. Theoretical calculations give, to an order of magnitude, good agreement with measured values. Scattered light has also been detected close to the direct beam.

The authors wish to thank Dr. J. C. Vial for his continued interest and helpful discussions.

<sup>1</sup>L. T. Canham, Appl. Phys. Lett. **57**, 1046 (1990).

<sup>2</sup>G. Vincent, Appl. Phys. Lett. **64**, 2367 (1994).

<sup>3</sup>V. Pellegrini, A. Tredicucci, C. Mazzoleni, and L. Pavesi, Phys. Rev. B **52**, R14328 (1995).

<sup>4</sup>G. L  rondel, R. Romestain, J. C. Vial, and M. Th  nissens, Appl. Phys. Lett. **71**, 196 (1997).

<sup>5</sup>A. Loni, L. T. Canham, M. G. Berger, R. Arens-Fischer, H. M  nder, H. L  th, H. F. Arrand, and T. M. Benson, Thin Solid Films **276**, 143 (1996).

<sup>6</sup>M. Araki, H. Koyama, and N. Koshida, Appl. Phys. Lett. **68**, 2999 (1996).

<sup>7</sup>H. F. Arrand, T. M. Benson, A. Loni, R. Arens-Fischer, M. G. Kr  ger, M. Thonissen, H. L  th, S. Kershaw, and N. N. Vorozov, J. Lumin. **80**, 119 (1999).

<sup>8</sup>H. F. Arrand, T. M. Benson, P. Sewell, A. Loni, R. J. Bozeat, R. Arens-Fischer, M. Kr  ger, M. Thonissen, and H. L  th, IEEE J. Sel. Top. Quantum Electron. **4**, 975 (1998).

<sup>9</sup>G. Vincent, F. Leblanc, I. Sagnes, P. A. Badoz, and A. Halimaoui, J. Lumin. **57**, 217 (1993).

<sup>10</sup>J. von Behren, L. Tsybeskov, and P. M. Fauchet, Appl. Phys. Lett. **66**, 1662 (1995).

<sup>11</sup>L. A. Balagurov, D. Yarkin, E. A. Petrova, A. F. Orlov, and S. N. Karyagin, Appl. Phys. Lett. **69**, 2852 (1996).

<sup>12</sup>D. Kovalev, G. Polisski, M. Ben-Chorin, J. Diener, and F. Koch, J. Appl. Phys. **80**, 5978 (1996).

<sup>13</sup>A. C. Boccara, D. Fournier, and J. Badoz, Appl. Phys. Lett. **36**, 130 (1980).

<sup>14</sup>S. Setzu, P. Ferrand, and R. Romestain, Mater. Sci. Eng., B **69–70**, 34 (2000).

<sup>15</sup>E. Daub and P. W  rfel, Phys. Rev. Lett. **74**, 1020 (1995).

<sup>16</sup>P. K. Tien, R. Ulrich, and R. J. Martin, Appl. Phys. Lett. **14**, 291 (1969).

<sup>17</sup>G. L  rondel, R. Romestain, and S. Barret, J. Appl. Phys. **81**, 6171 (1997).

<sup>18</sup>P. K. Tien, Appl. Opt. **10**, 2395 (1971).

<sup>19</sup>H. G. Unger, *Planar Optical Waveguides and Fibres* (Clarendon, Oxford, 1977).

<sup>20</sup>G. Allan, C. Delerue, M. Lannoo, and E. Martin, Phys. Rev. B **52**, 11982 (1995).

<sup>21</sup>H. M  nder, C. Andrzejak, M. G. Berger, U. Klemradt, H. L  th, H. H  rino, and M. Ligeon, Thin Solid Films **221**, 27 (1992).

<sup>22</sup>T. M. Benson, H. F. Arrand, P. Sewell, D. Niemeyer, A. Loni, R. J. Bozeat, M. Kr  ger, R. Arens-Fischer, M. Th  nissens, and H. L  th, Mater. Sci. Eng., B **69–70**, 92 (2000); N. Vorozov, L. Dolgyi, V. Yakovtseva, V. Bondarenko, M. Balucani, G. Lamedica, A. Ferrari, G. Vitran  , J. E. Broquin, T. M. Benson, H. F. Arrand, and P. Sewell, Electron. Lett. **36**, 722 (2000).

<sup>23</sup>S. Setzu, G. L  rondel, and R. Romestain, J. Appl. Phys. **84**, 3129 (1998).